Joanna SZELĄGOWSKA[1], Damian BISEWSKI[1], Janusz ZARĘBSKI[1],

Gdynia Maritime University, Department of Marine Electronics (1)

doi:10.15199/48.2020.02.42

Measurements of transient thermal impedance of SiC BJT

Abstract. *The paper presents the computer-aided method of measuring of the transient thermal impedance of SiC BJTs. The advantages of this method are illustrated by means of measurements of the silicon carbide BJT operating at the different cooling conditions.*

Streszczenie *W pracy przedstawiono komputerową metodę pomiaru przejściowej impedancji termicznej tranzystora SiC BJT. Zalety tego sposobu zilustrowano za pomocą pomiarów tranzystora SiC BJT pracującego w różnych warunkach chłodzenia. (**Pomiary przejściowej impedancji termicznej tranzystora SiC BJT**)*

Keywords: BJT, transient thermal impedance, thermal resistance, silicon carbide.
Słowa kluczowe: przejściowa impedancja termiczna, rezystancja termiczna, tranzystor bipolarny, węglik krzemu.

Introduction

Silicon carbide (SiC) is a promising wide bandgap material for high voltage and high temperature applications that meets still increasing requirements for semiconductor materials to produce high power devices [1-3]. Since last decade the market has been offering high-voltage silicon carbide bipolar power transistors (BJTs) [4].

Increase of a device internal temperature, resulting from the selfheating phenomenon, as well as an increase of the ambient temperature have a visible impact on the characteristics of a semiconductor devices including SiC power BJTs [5]. This must be correctly considered for an accurate modeling and also to ensure reliability. So, it is necessary to estimate the thermal parameters of these devices.

The transient thermal impedance $Z_{th}(t)$ of a device describes the device thermal properties, defined as a thermal response of the device for the Heaviside step function of the power and is defined by [6]:

$$Z_{thj-a}(t) = \frac{T_j(t) - T_a}{p_{th}(t)} \quad (1)$$

where: $T_j(t)$ – the internal temperature of the device (the junction temperature), Ta – the ambient temperature, $p_{th}(t)=P_0 \cdot 1(t)$ denotes the device dissipated power

The popular and commonly used model of the internal to ambient transient thermal impedance is of the form [6, 11– 5]:

$$Z_{thj-a}(t) = R_{thj-a} \cdot \left[1 - \sum_i a_i \cdot \exp\left(-\frac{t}{\tau_i}\right)\right] \quad (2)$$

where: $R_{thj-a}=Z_{thj-a}(t)|_{t\to\infty}$ - the junction-to-ambient thermal resistance, the sum of a_i is equal to 1, τ_i – the thermal time constant

The paper presents the computer-aided method of measuring of the transient thermal impedance and the thermal resistance of SiC BJT. This method is commonly used for measuring the considered parameters of many types of semiconductor devices, e. g. p-n, Schottky and LED diodes, transistors: IGBTs, JFETs, MOSFETs and MESFETs [7–12].

The results of a measurements of thermal parameters of the considered transistor working without a heat sink, and also placed on a heat sink at different values of the ambient temperature, are presented and discussed.

Measuring method

In the considered method, the base-to-emitter voltage v_{BE} of a forward biased pn junction of the transistor is used as a temperature sensor [16].

The measuring method consists of three major steps. In the first step, calibration of the $v_{BE}(T_a)$ isothermal characteristic of base-to-emitter (B-E) junction at relatively small fixed value of measuring current I_M is performed. During this process the internal device temperature is almost equal to the ambient temperature (selfheating phenomenon does not appear). Additionally, the slope of considered characteristic is calculated by the form $f=dv_{BE}/dT_a$. In the second step, heating of the tested transistor using current I_H is carried out. This step of a measurement is finished, when the device thermally steady state is achieved.

In the third step, measurements of the transient thermal impedance based on the cooling curve of the considered device [13,17], are performed. During the heating interruption, the automatically repeated measurements of the B-E junction voltage are carried out till the isothermal condition ($T_j \approx T_a$) is achieved. Due to the varied rate of a temperature changes during cooling of the tested transistor, measurements at several time intervals with different frequency values, are performed. The total heat-flow path between the transistor junction and the ambient is complicated and contains many different (in terms of construction and material) heat-transporting elements. Therefore, during the dissipation of a thermal power in the semiconductor device, very strong as well as slow temperature changes are observed. The fastest changes were observed in the case of a heat transfer from the elements with the smallest geometric dimensions (from the device junction to the leads), inversely than in the case of elements with larger dimensions (from the element case to the heat sink). Therefore, for the purposes of measuring thermal parameters, it is necessary to carry out measurements of the considered parameters with a different time steps, as shown in the table 1.

Table 1. Frequencies of the v_{BE} voltage measurement assigned to each time sections (third step)

Time section	Frequency
0 ÷ 16 ms	12500 Hz
16 ms ÷ 220 ms	1000 Hz
220 ms ÷ 2,2 s	100 Hz
2.2 s ÷ 22 s	10 Hz
22 s ÷ 300 s	1 Hz
300 s ÷ ∞	0.1 Hz

The diagram of the measuring set is presented in figure 1.

In the considered measuring system, the data acquisition device USB-1608GX manufactured by Measurement Computing was applied [18] in the connection to the PC computer. This device is equipped with the 16-bit analogue-to-digital converter for recording the voltage v_{BE} of

the tested BJT transistor, as well as a digital-to-analog converter controlling the operation of the switch S.

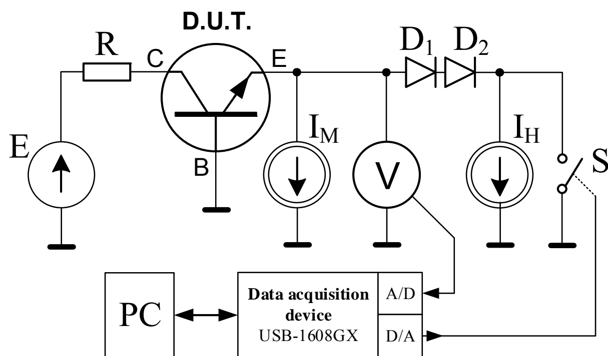

Fig. 1. Diagram of the measuring system

The source I_M forces the measuring current of forward biased B-E junction of the tested transistor (D.U.T.). The voltage source E as well as the current source I_H determine the dissipated power during the heating process. Diodes D_1 – D_2 eliminate undesirable influence of the heating current I_H on the I_M measuring current during the heating is being cut off.

In the case where the switch S is switched off, the transistor is being heated, whereas the coordinates of the transistor's operating point depend mainly on the efficiency of the voltage source E and the current source I_H. Otherwise, the I_H source is being cut off, and only the measuring current I_M flows through the base-emitter junction of the considered transistor.

The waveform of a temperature as a function of time $T_j(t)$ is being recorded by using the PC computer, while the internal to ambient transient thermal impedance $Z_{thj-a}(t)$ is calculated using equation (1).

Results of measurements

The thermal parameters of the BT1206AC SiC power BJT placed in TO-247 case and operating without a heat-sink, as well as situated on a small RAD-A5723/50-AL heat-sink of the dimensions equal to 35x50x78 mm, at the different values of the ambient temperature, have been performed by means of the presented method of the measurements. The catalog parameter values of the considered transistor are given in table 2 [19]. The manufacturer did not provide the value of the junction-to-case thermal resistance R_{thjc}.

Table 2. The catalog parameter values of the BT1206AC transistor

Parameter	Catalog value
V_{CEmax}	1200 V
I_{Bmax}	1 A
I_{Cmax}	6 A
T_{jmax}	175°C

The current-voltage isothermal input characteristics of B-E junction operating in the forward range, measured at four fixed ambient temperature values are shown in figure 3.

As it is presented (Fig. 3), the increase of the ambient temperature results in decreasing of the v_{BE} voltage value in all range of the base current shown in the figure.

As a result of the first measurement method step, the thermometric characteristic $v_{BE}(T_a)$ of the B-E junction at the fixed value of the measuring current I_M equal to 5 mA based on the measurements (Fig. 3) is shown in figure 4. The dependence of the v_{BE} voltage versus ambient temperature is linear, whereas the slope of the considered thermometric characteristic is equal to -2.1 mV/°C.

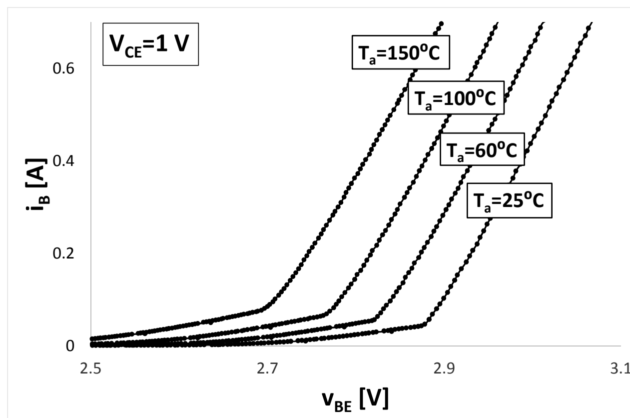

Fig. 3. Isothermal input characteristics of the B-E junction of the BT1206AC transistor

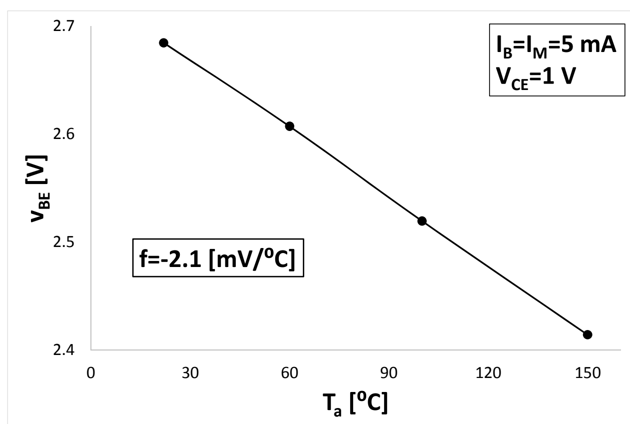

Fig. 4. Dependence of the v_{BE} voltage on the ambient temperature

The results of a measurements of the transient thermal impedance at a different values of the dissipated power are presented in figure 5.

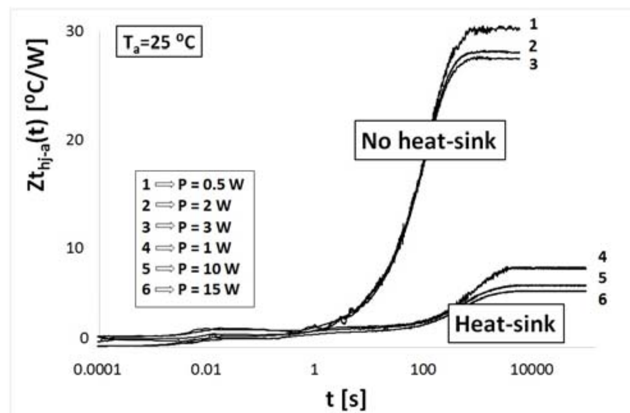

Fig. 5. Results of a measurements of the thermal impedance $Z_{thj-a}(t)$

As seen from figure 5, for the transistor operating without a heat-sink and situated on the heat sink, the thermal steady state appears after approximately 600 s and 4000 s, respectively. Measured values of the thermal resistance depend on the dissipated power and are significantly higher for the transistor operating without the heat-sink.

In practice, thermal models are used to determine the real-time internal temperature of the device [19,21-23]. These models are described as an electrical analog for

transient thermal impedance, in the form of a precisely defined combination of a resistance and thermal capacity, for example in the form of the Foster and Cauer networks thermal models [13,15,24-25]. Topologies of these models are shown in figure 6a and b respectively.

Elements R_1 - R_n and C_1 - C_n from Fig. 6 represent the thermal properties of individual structural elements of the transistor and additional elements (e.g. heat sink) that create heat-flow paths. The number of R_i and C_i segments is equal to the thermal time constants number in formula (2). The efficiency of the current controlled source G_{Pth} corresponds to the thermal power output in the transistor, while the efficiency of the independent voltage source V_{TA} represents the value of the ambient temperature. The internal temperature of the semiconductor element corresponds to the voltage at the node T_j [15, 26-30].

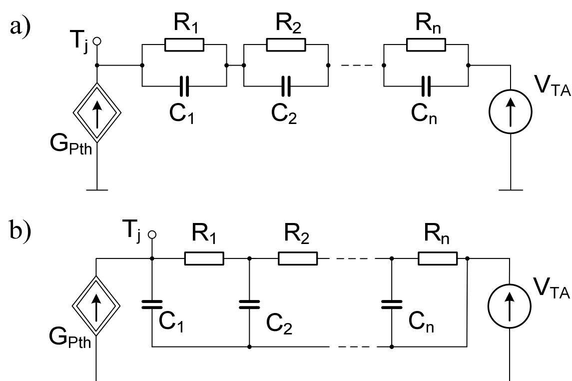

Fig. 6. Topology of the Foster (a) and Cauer (b) network thermal model

The values of R_i and C_i elements in the Foster network thermal model from Fig. 6a are determined by calculations based on the measured transient thermal impedance waveforms. The values of these elements are calculated from the equations 3-4 [15,26]:

$$R_i = a_i \cdot R_{th} \quad (3)$$

$$C_i = \tau_{hi} / R_i \quad (4)$$

where the semiconductor device thermal resistance R_{th} is equal to the sum of the resistance from R_1 to R_n according to the equation 5 [15, 26]:

$$R_1 + R_2 + \ldots + R_n = R_{th} \quad (5)$$

In the case of the Cauer network thermal model (Fig. 6b), the values of elements R_i and C_i appearing in the topology of this model are determined on the basis of the Foster model parameters [15,26].

The values of the transient thermal impedance model parameters a_i and τ_i described by the equation 2, were estimated using the computer program ESTYM reported in work [20]. Values of the coefficients obtained from the estimation procedure for the curves shown in figure 5 are presented in table 3.

As seen, the computer program designated three thermal time constants for curve 1, four thermal time constants for curves 2-4 and six thermal time constants for curves 5-6. The largest number of the thermal time constants have been designated for high power operation on the heat sink. As it is presented, the number of the thermal time constants increases with the number of elements in the heat-flow path.

Table 3.The estimated values of the coefficients for the curves from figure 5

Par.	The curve number (Fig. 5)					
	1	2	3	4	5	6
a_1	0.852	0.734	0.780	0.765	0.482	0.460
a_2	0.100	0.189	0.127	0.049	0.219	0.272
a_3	0.048	0.049	0.035	0.152	0.077	0.089
a_4	-	0.028	0.058	0.034	0.111	0.123
a_5	-	-	-	-	0.079	0.052
a_6	-	-	-	-	0.015	0.004
τ_{th1}	134.9	138.4	128.0	796.2	940.3	917.8
τ_{th2}	6.91	54.66	44.06	1.165	250.9	244.8
τ_{th3}	4E-5	4.047	4.032	0.003	0.977	0.822
τ_{th4}	-	0.002	4E-5	4E-5	0.018	0.025
τ_{th5}	-	-	-	-	0.002	4E-4
τ_{th6}	-	-	-	-	0.001	4E-5

Furthermore, the characteristics of the thermal resistance R_{thj-a} at the thermal steady state versus dissipated power p_H measured at three different values of the ambient temperature for the transistor operating without a heat-sink and placed on the heat-sink, are shown in figure 7 and 8, respectively.

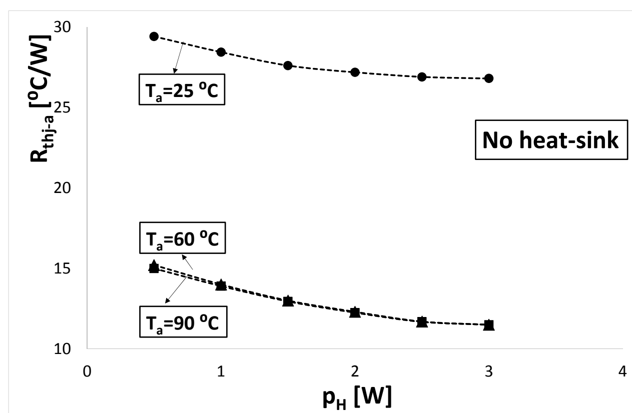

Fig. 7. The characteristics of the thermal resistance R_{thj-a} versus dissipated power p_H for the transistor operating without a heat-sink

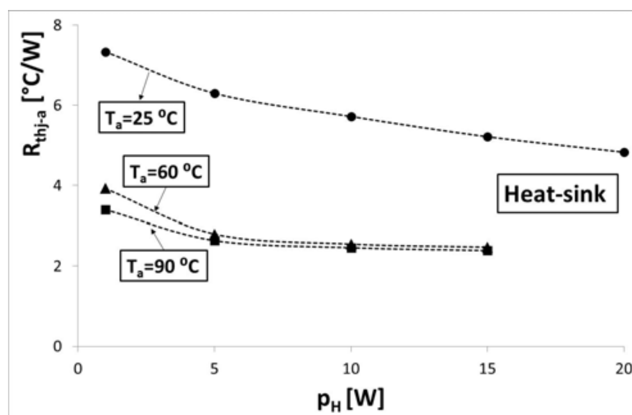

Fig. 8. The characteristics of the thermal resistance R_{thj-a} versus dissipated power p_H for the transistor placed on the heat-sink

As seen, the increase of the dissipated power results in decreasing of the R_{thj-a} value. For the ambient temperature value range up to approximately 60°C a dependence of the $R_{thj-a}(p_H)$ is a monotonically decreasing function, while for higher values of this power no significant changes of the thermal resistance value are observed.

In addition, the thermal resistance in the thermal steady state value at the ambient temperature equal to 25°C and for the dissipated power value equal to 1 W is almost four times lower in the case of the transistor placed on a heat-sink compared to the transistor without a heat-sink.

Conclusion

The results of the measurements of the transient thermal impedance as well as the thermal resistance values of the SiC BJT at different cooling conditions, have been presented. In the measurements a computer aided measuring system has been used. The values of the thermal parameters strongly depend on the dissipated power, ambient temperature and cooling conditions. As an example, value of the thermal resistance at the ambient temperature equal to 25°C is approximately over four times higher than for the transistor operating with the heat-sink. It also turns out that in the transient thermal impedance model, a greater number of thermal time constants are required to describe the thermal properties of the transistor operating on the heat sink which results from a more complex heat flow from the inside of the element to the ambient.

In future investigations the non-linear compact thermal model of SiC BJTs will be elaborated which will be used to develop the electro-thermal SPICE model of the considered class of devices.

***Authors**: mgr inż. Joanna Szelągowska, Gdynia Maritime University, Department of Marine Electronics, 83 Morska Str., 81-225 Gdynia, e-mail: j.szelagowska@we.umg.edu.pl; dr inż. Damian Bisewski Gdynia Maritime University, Department of Marine Electronics, 83 Morska Str., 81-225 Gdynia, e-mail: d.bisewski@we.umg.edu.pl; prof. dr hab. inż. Janusz Zarębski Gdynia Maritime University, Department of Marine Electronics, 83 Morska Str., 81-225 Gdynia, e-mail: j.zarebski@we.umg.edu.pl,*

REFERENCES

[1] She X., Huang A.Q., Lucía Ó., Ozpineci B., *Review of Silicon Carbide Power Devices and Their Applications,* IEEE Transactions on Industrial Electronics, Vol. 64, Issue 10, pp. 8193-8205,2017

[2] Wang J., Liang S. Deng L., Yin X., Shen Z.J., *An Improved SPICE Model of SiC BJT Incorporating Surface Recombination Effect,* IEEE Transactions on Power Electronics Vol. 34 , Issue 7, pp. 6794 – 6802, 2019

[3] Liang S., Wang J., Peng Z., Chen G., Yin X. Shen Z.J., Deng L., *A Modified Behavior SPICE Model for SiC BJT,* Annual IEEE Applied Power Electronics Conference and Exposition, Proceedings Paper, pp. 238-243, 2018

[4] Patrzyk J., Bisewski D., *Measurements and simulations of silicon carbide current-controlled transistors*, 21st European Microelectronics and Packaging Conference (EMPC) & Exhibition, Poland, 2017

[5] Szelagowska J., *Characteristics and parameters of power SiC SJT,* Przegląd Elektrotechniczny, Vol. 94, Issue 8, pp. 75-78, 2018

[6] Górecki K., Zarębski J., *Modeling the Influence of Selected Factors on Thermal Resistance of Semiconductor Devices,* IEEE Transactions on Components, Packaging and Manufacturing Technology, Vol. 4, Issue 3 , 2014

[7] Bargieł K., Bisewski D., Zarębski J, *Modelling of SiC-JFET in PSPICE*, Przegląd Elektrotechniczny, Vol.95, Issue 1, pp.231-234, 2019

[8] Górecki K., Ptak P., *New dynamic electro-thermo-optical model of power LEDs*, MicroElectronics Reliability, Vol. 91, pp. 1-7

[9] Górecki K., Górecki P., *A new form of non-linear compact thermal model of the IGBT,* 12th International Conference on Compatibility, Power Electronics and Power Engineering (CPE-POWERENG 2018), Qatar

[10] Zarębski J., Dąbrowski J., *Non-isothermal Characteristics of SiC Power Schottky Diodes,* International Symposium on Power Electronics, Electrical Drives, Automation and Motion, Vols 1-3, Pages: 1363-1367, 2008, Italy

[11] Smirnov V.I., Sergeev V.A., Gavrikov A.A.,Shorin A.M., *Thermal Impedance Meter for Power MOSFET and IGBT Transistors*, IEEE Transactions On Power Electronics, Vol. 33, Issue 7, pp.6211-6216, 2018

[12] Blackburn D. L., Oettinger F. F., *Transient Thermal Response Measurement of Power Transistors*, IEEE Transactions on Industrial Electronics and Control Instrumentation, Vol. IECI-22, No. 2, 1975, pp. 134-141.

[13] Górecki K., Górecki P., Zarębski J., *Measurements of Parameters of the Thermal Model of the IGBT Module*, IEEE Transactions on Instrumentation and Measurement (Early Access), pp.1-12, 2019

[14] Janicki M., Sarkany Z., Napieralski A., *Impact of nonlinearities on electronic device transient thermal responses*, Microelectronics Journal, Vol. 45, Issue 12, pp.1721-1725, 2014

[15] Szekely V., *A New Evaluation Method Thermal Transient Measurements Results*, Microelectronics Journal, Vol. 28, No. 3, 1997, pp.277-292

[16] Starzak Ł., Stefanskyi A., Zubert M., Napieralski A., *Improvement of an electro-thermal model of SiC MPS diodes,* IET Power Electronics, Vol. 11, Issue 4, pp. 660–667, 2018

[17] Du X., Zhang J., Zheng S., Tai H-M., *Thermal Network Parameter Estimation Using Cooling Curve of IGBT Module,* IEEE Transactions on Power Electronics, Vol. 34, Issue 8, pp. 7957 – 7971, 2019

[18] https://www.mccdaq.com/usb-data-acquisition/USB-1608G-Series.aspx

[19] http://www.dacpol.eu/pl/elementy-polprzewodnikowe-z-weglika-krzemu/product/elementy-polprzewodnikowe-z-weglika-krzemu-1224

[20] Zarębski J., Górecki K., *Parameters Estimation of the D.C. electrothermal model of the bipolar transistor*, International Journal of Numerical Modelling: Electronic Networks, Devices and Fields, Vol. 15, Issue 2, pp. 181-194, 2002

[21] Bąba S., Zelechowski M., Jasiński M., *Estimation of thermal network models parameters based on particle swarm optimization algorithm,* Conference Paper, CPE-POWERENG 2019 13th International Conference on Compatibility, Power Electronics and Power Engineering, 2019

[22] Riccio M., De Falco G., Mirone P., Maresca L., Tedesco M., Breglio G., Irace A., *SPICE Modeling of Reverse-Conducting IGBTs Including Self-Heating Effects, IEEE Transactions on Power Electronics, Vol. 32 , Issue 4 ,pp. 3088 – 3098, 2017*

[23] Du B., Hudgins J.L., Santi E., Bryant A.T., Palmer P.R., Mantooth H.A., *Transient Electrothermal Simulation of Power Semiconductor Devices,* IEEE Transactions on Power Electronics, Vol. 25, Issue 1, pp. 237–248, 2010

[24] Boglietti A., Carpaneto E., Cossale M., Vaschetto S., *Stator-Winding Thermal Models for Short-Time Thermal Transients: Definition and Validation,* IEEE Transactions on Industrial Electronics Vol. 63 , Issue 5, pp. 2713 – 2721, 2016

[25] Bonyadi R., Alatise O., Jahdi S., Hu J., Gonzalez J.A.O., Ran L., Mawby P.A., *Compact Electrothermal Reliability Modeling and Experimental Characterization of Bipolar Latchup in SiC and CoolMOS Power MOSFETs,* IEEE Transactions on Power Electronics, Vol. 30 , Issue 12, pp. 6978 – 6992, 2015

[26] Bagnoli P.E., Casarosa C., Ciampi M. and Dallago E., *Thermal Resistance Analysis by Induced Transient Method for Power Electronic Devices Thermal Characterization* – Part I: Fundamentals and theory, IEEE Transactions on Power Electronics, Vol. 13, no. 6, , pp.1208-1219, 1998

[27] Masana F.N., *Extraction of structural information from thermal impedance measurements in time domain*, Proceedings of the 18th International Conference Mixed Design if Integrated Circuits & Systems MIXDES 2011, Gliwice, pp.398-402

[28] Mawby P.A., Igic P.M., and Towers M.S., *Physically based compact device models for circuit modelling applications*, Microelectronics Journal, Vol.32, pp.298-302, 2001

[29] d'Alessandro V., Pio Catalano A., Codecasa L., Moser B., Zampardi P.J., *Thermal Coupling in Bipolar Power Amplifiers toward Dynamic Electrothermal Simulation*, 2018 IEEE MTT-S International Conference on Numerical Electromagnetic and Multiphysics Modeling and Optimization (NEMO)

[30] Sheng K., *Maximum Junction Temperatures of SiC Power Devices,* IEEE Transactions on Electron Devices, Vol. 56, Issue 2, pp. 337-342, 2009